

Organic/Inorganic bioactive materials Part III: *in vitro* bioactivity of gelatin/ silicocarnotite hybrids

Research Article

Lachezar Radev^{1*}, Maria Helena V. Fernandes², Isabel Miranda Salvado²,
Daniela Kovacheva³

¹Department of Chemical Technology, University of Chemical Technology and Metallurgy, Sofia, 1756 Bulgaria

²Department of Ceramic and Glass Engineering and CICECO, University of Aveiro, Aveiro, 3810-193 Portugal

³Institute of General and Inorganic Chemistry, Bulgarian Academy of Sciences, Sofia, 1113 Bulgaria

Received 30 April 2009; Accepted 18 June 2009

Abstract: In this work we present our experimental results on synthesis, structure evolution and *in vitro* bioactivity assessment of new gelatin/silicocarnotite hybrid materials. The hybrids were obtained by diluting gelatin (G) and silicocarnotite (S) ceramic powder with G:S ratios of 75:25 and 25:75 wt.% in hot (40°C) water. The hybrids were characterized using XRD, FTIR, SEM/EDS and XPS. FTIR depicts that the “red shift” of amide I and COO⁻ could be attributed to the fact that the gelatin prefers to chelate Ca²⁺ from S. The growth of calcium phosphates on the surface of the hybrids synthesized and then immersed in 1.5 SBF for 3 days was studied by using of FTIR, XRD and SEM/EDS. According to FTIR results, after an immersion of 3 days, A and B-type CO₃HA can be observed on the surface. XRD results indicate the presence of hydroxyapatite with well defined crystallinity. SEM/EDS of the precipitated layers show the presence of CO₃HA and amorphous calcium phosphate on the surface of samples with different G/S content when immersed in 1.5 SBF. XPS of the G/S hybrid with 25:75 wt.% proved the presence of Ca-deficient hydroxyapatite after an *in vitro* test for 3 days.

Keywords: Gelatin • Silicocarnotite • Hybrids • *In vitro* bioactivity
© Versita Warsaw and Springer-Verlag Berlin Heidelberg.

1. Introduction

For the significant part of clinical applications bioamaterials should be porous, biodegradable and promote new bone formation. Hard tissues are composed of both inorganic and organic phases. For creation of biological bone Chang and DeLong [1] point out the presence of three fundamental structural factors: hydroxyapatite (HA) nanocrystals, collagen and organic/inorganic interaction between them. Hydroxyapatite (HA) is the main inorganic component of hard tissues such as bone and teeth, in the human body [2-4]. The organic phase consist of type I collagen and small amounts of

proteoglycans, glycoproteins and glucosaminoglycans. As is known, gelatin is a denaturated form of collagen and contains a number of biological functional groups, making it suitable for hard tissue application.

Nanostructured HA offers a favourable environment for osteoconduction, protein adhesion and bone regrowth [5,6]. Much of the research interests today focus on the fabrication of artificial bone like ceramic/polymer composites [6-9] especially on HA/gelatin nanocomposites [1,10-22], fluorapatite (FHA)/gelatin nanocomposites [23], carbonated fluorapatite (CO₃FHA)/gelatin nanocomposites [24]; drug delivery carrier [25,26] and protein separation [27].

* E-mail: l_radev@abv.bg

Lien *et al.* [28] tried to show the feasibility of the ceramic-gelatin assembly (CGA) scaffolds for articular cartilage repair. The ceramic components of the hybrids obtained were tricalcium phosphate (TCP) and amorphous calcium polyphosphate (ACCP), respectively. Panzavolta *et al.* [29] prepared gelatin foams that contained increasing amounts (up to 40 wt.%) of TCP. The hybrid material obtained was produced in the presence of non-toxic crosslinking agent-genipine. They concluded that a partial hydrolysis of α -TCP to octacalcium phosphate (OCP) occurs during the foaming process of freeze-drying. A biodegradable gelatin/TCP composite composed of oligomeric proanthocyanidins cross-linked gelatin mixed with TCP was developed by Chen *et al.* [30] as a bone substitute.

In recent years some authors have even prepared silicon substituted hydroxyapatites (SiHA) *via* sol-gel method using TEOS as a SiO_2 precursor for glass-ceramic samples [31-33]. In the materials so synthesized, they found other crystalline phases, such as TCP and CaO. It is known that silicocarnotite is a calcium silicophosphate with carnotite structure. Some authors determined that the silicocarnotite structure is very similar to hydroxyapatite and examined its *in vitro* bioactivity [34]. They concluded that the introduction of silicon in HA lattice improved *in vitro* bioactive response as compared to the apatite without silicon content [34]. Others suggested that the loss of all -OH from HA due to SiO_4 substitution results in silicocarnotite structure. They considered silicocarnotite as a mixture of a silicon substituted dehydrated apatite and oxyapatite [35]. Ruys [31] found that the silicocarnotite can be present as a impurity phase in HA structures at the lowest SiO_2 addition accompanied by increasing amounts of a α - and β -TCP in Ca-Si-P-O amorphous phase.

In our previous works, on the basis of sol-gel method we synthesized some bioactive ceramic systems, $\text{CaO-SiO}_2\text{-P}_2\text{O}_5$ [36] and $\text{CaO-SiO}_2\text{-P}_2\text{O}_5\text{-MgO}$ [37]. The materials synthesized were shown to have an *in vitro* bioactivity when evaluated in 1.5 SBF. With the ceramic powders as the base, we synthesized *in vitro* bioactive hybrid materials in the presence of collagen [38,39]. In other papers we used bioactive glasses in the $\text{SiO}_2\text{-3CaO-P}_2\text{O}_5\text{-MgO}$ [40], $\text{P}_2\text{O}_5\text{-CaO-Na}_2\text{O-K}_2\text{O}$ [41], and fluorapatite (FA)- MgO-SiO_2 and $\text{FA-MgO-Al}_2\text{O}_3\text{-SiO}_2$ gel glasses [42] for obtaining new composites that showed interesting applications. New nanostructured hybrid materials containing Al_2O_3 for alumina-silica oxycarbonitride materials and hybrid systems Si-O-C-N-Zr have been synthesized in the presence of different silica precursors [43,44]. On the

other hand we have also investigated the influence of different silica precursors on the structure of hybrid materials in the presence of HEMA, PEO and Chitin for cell immobilization [45].

The purpose of this study was to develop new bioactive materials with silicocarnotite ceramics by addition of gelatin. The experimental methodology comprised of three main steps. In the first step, silicocarnotite was fabricated *via* polystep sol-gel method, as described in [36]. The second step involved preparation of gelatin/silicocarnotite hybrids in 25:75 and 75:25 wt.% by soft chemical route. Finally, the hybrid materials obtained were soaked in 1.5 SBF for assessment of *in-vitro* bioactivity.

2. Experimental Part

2.1. Preparation of the silicocarnotite as the inorganic part of the synthetic hybrids

The silicocarnotite (S) was synthesized by polystep sol-gel method as described in [36].

2.2. Preparation of the gelatin/silicocarnotite hybrid materials

The gelatin/silicocarnotite (G/S) hybrids for 75:25 and 25:75 wt.% were prepared by adding the inorganic powder to the gelatin (Fluka). Gelatin was taken in amounts corresponding to the hybrid content and added to 30 mL of distilled water at 40°C and dissolved by stirring for 30 min at room temperature. Gelatin concentration in the solutions was calculated on the basis of 0.7 g weight of dry hybrid. After homogenization, the finely powdered S was added in the required amounts to the dissolved gelatin with continuing intensive stirring. The stirring time was 3 h, pH was adjusted at 8 using 25% NH_4OH and a volume of 0.5 mL 0.01% sodium azide was added to the mixed xerogel to prevent bacterial growth [46]. The hybrid materials obtained were dried in air at 37°C for 12 h.

2.3. *In vitro* assessment of bioactivity in 1.5 SBF

Bioactivity of G/S hybrids obtained was evaluated by examining apatite formation on their surfaces after immersion in 1.5 SBF.

The 1.5 SBF solution was prepared as a solution with 11.9925 g NaCl, 0.5295 g NaHCO_3 , 0.3360 g KCl, 0.3420 g $\text{K}_2\text{HPO}_4\cdot 3\text{H}_2\text{O}$, 0.4575 g $\text{MgCl}_2\cdot 6\text{H}_2\text{O}$, 0.5520 g $\text{CaCl}_2\cdot 2\text{H}_2\text{O}$, 0.1065 g Na_2SO_4 . The solution was then buffered at 36.5°C to a pH of 7.4 at with 9.0075 g TRIS and 1M HCl in distilled water. S/G hybrids were pressed

at 50 MPa with PVA to obtain disc specimens 12 mm in diameter and 2 mm thick that were then immersed in 1.5 SBF at the human body temperature of 36.6°C in polyethylene bottles and then maintained in static conditions for 3 days. After soaking, the specimens were removed from the fluid and gently rinsed with distilled water and dried at 37°C for 6 h [47].

2.4. Measurements and observations

The structure and *in vitro* bioactivity of G/S hybrids were monitored by XRD, FTIR, SEM/EDS and XPS.

Powder X-ray diffraction spectra were collected within the range of 10° to 80° 2θ with a constant step 0.04° 2θ and counting time 1s/step on a Bruker D8 Advance diffractometer with CuK_α radiation and SolX detector. The spectra were evaluated with the *Diffraclus* EVA package.

The composition and the electronic properties of the hybrids after *in vitro* testing in 1.5 SBF were investigated by X-ray photoelectron spectroscopy (XPS). The measurements were performed in a VG ESCALAB II electron spectrometer using AlK_α radiation with energy of 1486.6 eV. The binding energies (BE) were determined with an accuracy of ±0.1 eV utilizing the C1s line at 285.0 eV (from an adventitious carbon) as a reference. The composition and chemical surrounding of the films were investigated on the basis of the areas and binding energies of C1s, O1s, Ca2p, P2p, Si2p, Na1s, Cl2p and N1s photoelectron peaks (after linear subtraction of the background) and Scofield's photoionization cross-sections.

On the dry ceramic powders and organic/inorganic hybrids, FTIR transmission spectra were recorded using a Bruker Tensor 27 spectrometer with the scanner velocity at 10 KHz. KBr pellets were prepared by mixing ~1 mg of the samples with 300 mg KBr. Transmission spectra were recorded using MCT detector, with 64 scans and 1 cm⁻¹ resolution.

SEM (Jeol, JSM-35 CF, Japan) in conjunction with EDS at accelerating voltage of 10 kV was used to ascertain the morphology and chemical constituents of the hybrids after immersion in 1.5 SBF for 3 days.

3. Results and Discussion

3.1. X-ray diffraction of the synthesized hybrids, before *in vitro* test

Fig. 1 shows the X-ray diffraction patterns of pure gelatine, revealing that the structure is essentially amorphous with a more pronounced peak [48] at around 20° 2θ.

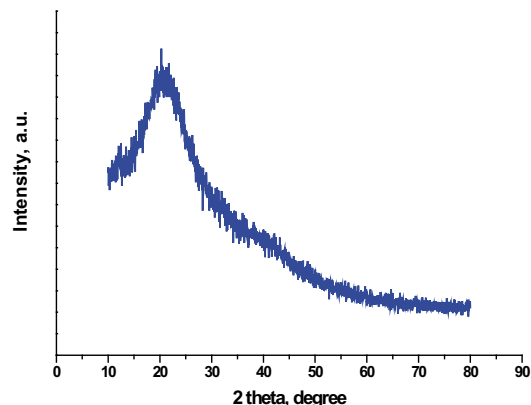


Figure 1. XRD of pure gelatin (Fluka)

X-ray diffraction data for the G/S hybrid material (25:75 wt.%) prepared is presented in Fig. 2.

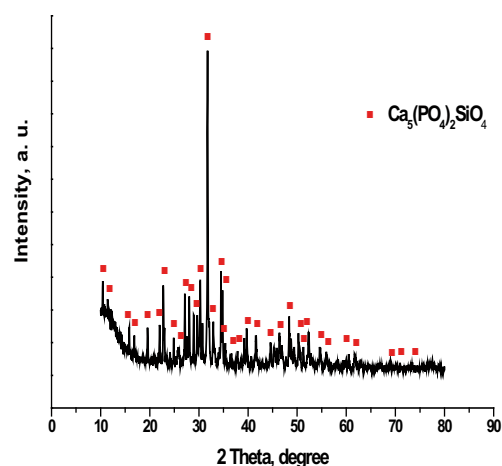


Figure 2. XRD of the prepared G/S hybrid (25:75 wt.%) sample

The phase of gelatin/silicocarnotite hybrid was analyzed by X-ray diffraction reflections, as shown in Fig. 2. In the hybrid material obtained, typical silicocarnotite (PDF 40-0309) peaks were observed [36]. In conclusion, we see that the gelatin/silicocarnotite hybrids provide well-defined signals with smaller peak width in spite of the presence of an amorphous phase. This suggests the association of crystalline silicocarnotite to an amorphous gelatin. The data obtained corresponds with the results of other authors [19].

3.2. FTIR of the synthesized G/S hybrids, prior to *in vitro* testing in 1.5 SBF

Fig. 3 represents the FTIR spectrum of pure gelatin, the organic part of the hybrids.

It is known that the amide groups of polypeptides and proteins possess characteristic vibration modes of group frequencies. The region of amide I, II and III bands of the spectrum are directly related to the polypeptide conformation [49]. The amide I band with the characteristic frequencies in the range 1600-1700 cm^{-1} is mainly associated with the stretching vibrations of the carbonyl groups (C=O bond) along the polypeptide backbone [15,23,50] and is a sensitive marker of the peptide secondary structure. Three typical bands at 1650-1660 cm^{-1} , 1630-1640 cm^{-1} and 1680-1700 cm^{-1} in the amide I region of the protein is well established. In the present case amide I band is centered at 1670 cm^{-1} [15,23]. The amide II region of the protein bands are observed at 1540-1550 cm^{-1} , 1620-1530 cm^{-1} and 1520-1545 cm^{-1} [51]. In pure gelatin the amide II is centered at 1547 cm^{-1} . For the amide III, there are bands centered at 1270-1300 cm^{-1} , 1229-1235 cm^{-1} and 1243-1253 cm^{-1} [15,23,24,51]. Fig. 3 shows a band assigned to the amide III at 1251 cm^{-1} , as described in [50]. Two bands at 1407 and 1340 cm^{-1} can be assigned to the presence of COOH and COO⁻ as seen in the spectrum of pure collagen and gelatin [10,15,23].

FTIR of the prepared G/S hybrids before the *in vitro* test are given in Figs. 4 and 5.

FTIR spectra depicted in Figs. 4 and 5 show very complicated data. In accordance with literature data [52,53], the intense bands centered at 568, 600, 960, 1043 and 1008 cm^{-1} correspond to ν_4 , ν_1 and ν_3 P-O stretching vibration modes. The FTIR spectra of the hybrid materials prepared, exhibit characteristic ν_3 PO₄³⁻ and ν_1 PO₄³⁻ bands indicated by the presence of three peaks at 1015, 1060 and 942 cm^{-1} (Figs. 4 and 5) [53]. On the other hand the absorption bands centred at 1015 (1080) cm^{-1} for the two samples can be assigned to the vibration of the Si-O-Si bond [54]. The ν_4 PO₄³⁻ was identified by the presence of some peaks posited at 548, 583, 615 and 689 cm^{-1} (Fig. 4) and 526, 549, 585, 615 and 689 cm^{-1} (Fig. 5) [53,55]. For the hybrid materials synthesized, the absorption peaks centered at 504, 845 and 942 cm^{-1} (Fig. 4) and 504, 875 and 942 cm^{-1} (Fig. 5) were observed. These peaks can be assigned to the presence of SiO₄⁴⁻ in the hybrids [55]. From the spectra we also see that the silicon content leads to a decrease in the intensity of the band centered at 630 cm^{-1} (for the two samples) that corresponds to the presence of -OH [36]. This observation is consistent with the silicon substitution

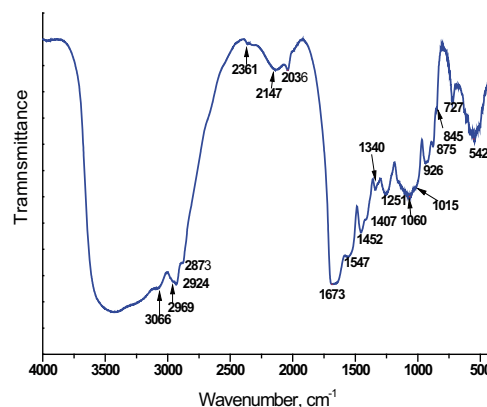


Figure 3. FTIR of pure gelatin

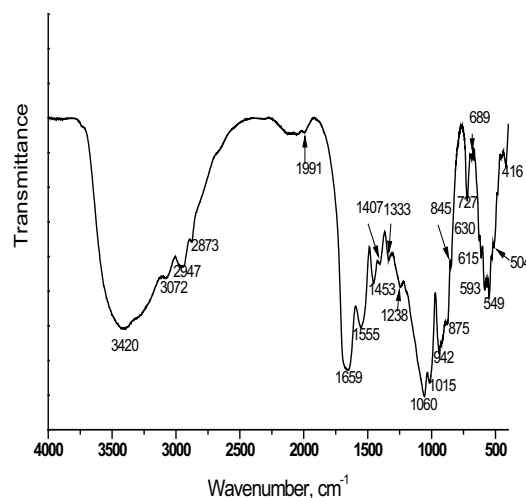


Figure 4. FTIR of G/S hybrid (75:25 wt.%) before immersion in 1.5 SBF

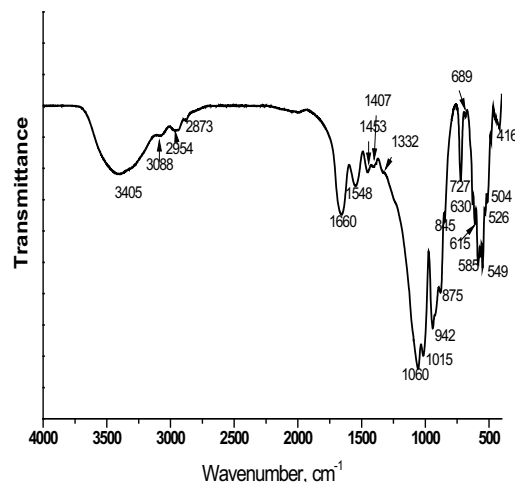


Figure 5. FTIR of G/S hybrid (25:75 wt.%) before immersion in 1.5 SBF

mechanism proposed as $\text{SiO}_4^{4-} \rightarrow \text{PO}_4^{3-}$, leading to loss of some -OH groups so as to maintain the charge balance [52]. From the FTIR results obtained we can assume that the inorganic part silicocarnotite, of the hybrids may be partially dehydroxylated [36]. This also explains the dramatic decrease of the OH stretches at 3404 cm^{-1} (Fig. 4) and 3420 cm^{-1} (Fig. 5) in samples with increasing addition of silicon [36].

Furthermore, there are two distinct changes when the spectra of pure gelatine (Fig. 3) and G/S hybrids with different weight ratio of the components (Figs. 4 and 5) were compared. First, the intensity of amide II had increased while that of the amide III had slightly decreased. Second, the amide I peak observed for pure gelatine centered at 1673 cm^{-1} (Fig. 3) shifted to 1658 cm^{-1} (Fig. 4) and to 1660 cm^{-1} (Fig. 5), respectively. From the FTIR spectra obtained we can conform that gelatine prefers to chelate Ca^{2+} from the partially dissolved silicocarnotite glass-ceramic under the conditions. We determined the partially dissolved silicocarnotite by the decrease in intensity of the $\nu\text{Si-O-Ca}$ band centered at 942 cm^{-1} [56]. Furthermore, FTIR spectrum (Fig. 4) shows that the flexible vibration of $\nu\text{Si-O}$ at 904 cm^{-1} became weak and the band, centered at 1060 cm^{-1} became sharp. The peak centered at 1015 cm^{-1} ($\nu \text{O-Si-O}$) slightly decreased. The analysis indicates that O-Si-O and Si-O-Ca groups are exposed and transferred under the experimental conditions. As can be seen, the “red shift” of amide I peak (Figs. 4 and 5) indicates that the C=O bonds in the peptide chain are weakened because of the formation of new chelate bonds between Ca^{2+} and C=O bond. Other researchers concluded that the carbonyl groups on the surface of peptide are binding sites of Ca^{2+} [57]. As reported earlier, since C=O has non-bonding free electron pairs it is therefore possible for carbonyl oxygen to chelate with some metal ions that have vacant electron orbitals [47].

The very interesting feature in the FTIR spectra (Figs. 4 and 5) is the presence of the band centred at $1333\text{-}332 \text{ cm}^{-1}$ that could be ascribed to the formation of $\text{COO}^-\text{Ca}^{2+}$ bond. As can be seen the asymmetric stretching vibration of the above carboxylate anions (COO^-), observed in pure gelatine and collagen at 1340 cm^{-1} shifted to lower wavenumber in the case of the hybrids (Figs. 4 and 5). The amount of “red shift” could be determined by the preparation conditions, such as pH and concentration of reagents [10]. In our case, the “red shift” is not influenced from the concentration of two different components of the hybrids.

It is worth mentioning that the chemical bond formation between COO^- and Ca^{2+} in the synthesized hybrid materials was not carried out under biomimetic

pathway as it was established by other authors [1,10,18-20,23,58]. It affords interesting opportunities in the field of hybrid materials, synthesized under soft conditions with the participation of calcium phosphate silicate glass ceramics. It would be interesting to know whether the above mentioned tendency concerning the participation of sol-gel glasses will be met. This will be an object of our future research

3.3. XRD and XPS of the obtained hybrid materials after immersion in 1.5 SBF

Fig. 6 depicts X-ray diffraction patterns of the G/S hybrids obtained after 3 days of immersion in 1.5 SBF.

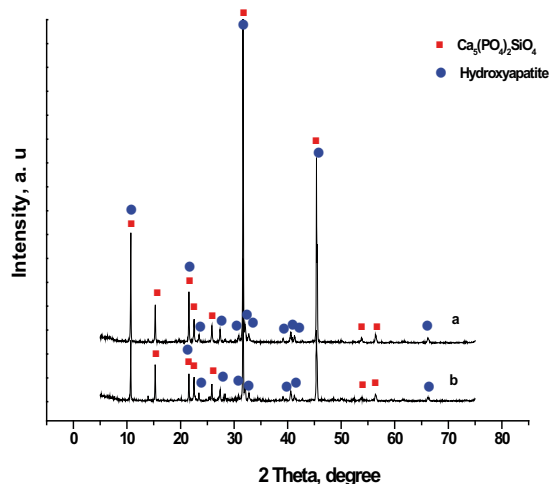


Figure 6. XRD obtained for G/S hybrid materials with 25:75 wt.% (a) and 75:25 wt.% (b) after immersion in 1.5 SBF for 3 days

The XRD pattern before (Fig. 2) and after (Fig. 6) immersion in 1.5 SBF is obviously quite different. The graph shows the presence of hydroxyapatite (PDF 76-0694) of defined crystallinity with the presence of crystallographic maxima at 10.6° , 32.2° , 32.8° and 45.5° 2θ (Fig. 6). We also see that the crystallinity of silicocarnotite phase slightly decreases after immersion in 1.5 SBF. Further, the intensity of the amorphous halo of gelatin also decreased after the immersion process. XPS analysis of the elements on the surface of the G/S hybrid synthesized with 75:25 wt.% and immersed in 1.5 SBF for 3 days is given in Fig. 7.

$\text{Ca}2p$, $\text{P}2p$, $\text{O}1s$, $\text{C}1s$ and $\text{N}1s$ were identified for the sample that was obtained after immersion process. Additional peaks of $\text{Na}1s$, $\text{Si}2p$ and $\text{Cl}2p$ were also found. The peak position of elements detected on the surface and their relative concentration is presented in Table 1.

As can be seen, the binding energies determined for P2p, Ca2p and O1s and obtained at 132.96 eV, 347.09 (350.44) eV (Fig. 8) and 531.2 eV undoubtedly corresponded to calcium phosphate (apatite) formation on the surface of the immersed samples. However, this apatite probably is calcium-deficient apatite

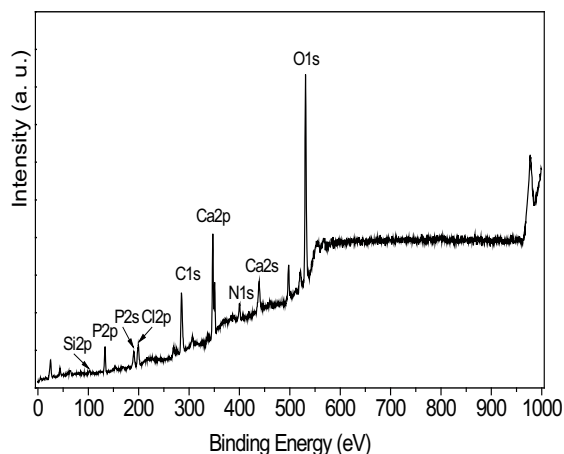


Figure 7. XPS spectrum for obtained G/S hybrid material 25:75 wt.% after immersion in 1.5 SBF for 3 days

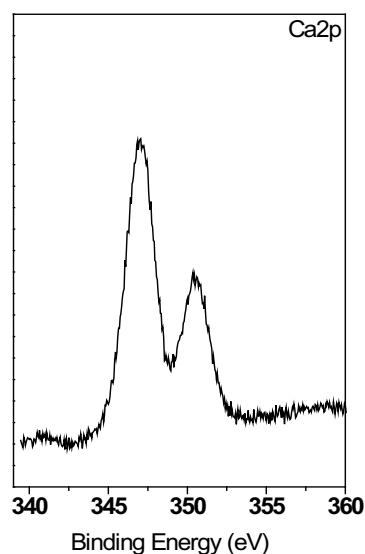


Figure 8. XPS Ca2p spectrum for G/S hybrid material 25:75 wt.% after immersion in 1.5 SBF for 3 days

layer because its Ca/P (at.%) was equal to 1.3. This ratio is much lower than the Ca/P of 1.67, the normal stoichiometric value. The C1s peak centred at 285.38 eV corresponded to the aliphatic or aromatic C atoms from amino acid residues of gelatine. The N1s posited at 400.1 eV could be ascribed to the presence of the nitrogen atom of the peptide backbone. The presence of Si2p, centered at 102.91 eV corresponds to processes of incomplete covering of hybrid surface with crystalline calcium phosphate coating (or even after three days).

3.4. FTIR of the prepared hybrids after immersion in 1.5 SBF for 3 days

FTIR data for the G/S samples after immersion in 1.5 SBF are presented in Figs. 9 and 10.

As can be seen, the spectra presented are similar to those of carbonated hydroxyapatite-protein composites, previously reported by other authors [59]. For the G/S hybrids obtained after immersion process, both the FTIR spectra (Figs. 9 and 10) exhibit the presence of ν_1 - ν_4 PO_4^{3-} modes [10,17,18,24,58,60,61]. For the two samples the infrared absorption bands of ν_2 CO_3^{2-} were found at 866 cm^{-1} with a shoulder at 872 cm^{-1} for G/S 25:75 wt.% (Fig. 10) [24,58,61], ν_3 CO_3^{2-} at 1466 cm^{-1} (Fig. 10) and 1460 cm^{-1} (Fig. 9) [24] and weak bands centered at 692 cm^{-1} (for two samples), which correspond to the B-type carbonate substitution ($\text{CO}_3^{2-} \rightarrow \text{PO}_4^{3-}$) in the hydroxyapatite lattice [10,19,24,61,62]. The two FTIR spectra display a band, centered at 1549 (1555) cm^{-1} , which can be attributed to the presence of A-type ($\text{CO}_3^{2-} \rightarrow \text{OH}^-$) carbonate substitution as well as to amide II [24,61]. This finding allows us to conclude the presence of CO_3^{2-} ions within the channels of the apatite crystal structure in aggregates grown in accordance with experimental conditions of reference [24]. On the other hand, Suetsugu *et al.* investigated and ascribed the peaks at $\sim 1460\text{ cm}^{-1}$ to ν_{3a} of A-site CO_3^{2-} and ν_{3b} of B-site CO_3^{2-} [63]. Additionally, amide A and B exhibit bands at 3070 - 3196 cm^{-1} which overlap with the stretching modes of the water molecules. Trace amount of -OH in apatite component of the samples subjected to the immersion process are indicated by the existence of weak bands at 692 cm^{-1} in the FTIR spectra (overlap with the ν_4

Table 1. Binding energy (eV) and relative concentration (at. %) of the elements detected on the surface of G/S hybrid material 75:25 wt.% after immersion in 1.5 SBF for 3 days

Characteristics	Elements								
	C	O	Ca	P	Si	Na	Cl	N	Ca/P
Binding energy, eV	285.38	531.2	347.05 350.35	132.96	102.91	1072.3	199.17	400.1	-
Relative concentration, at.%	29.4	35.6	12.3	9.0	1.7	1.9	6.6	3.5	1.36

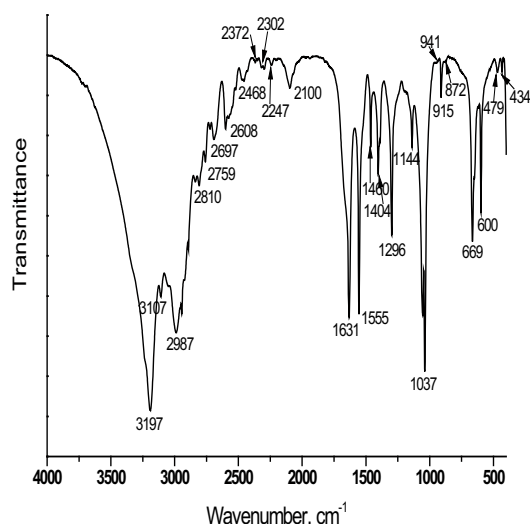


Figure 9. SEM of the G/S (75:25 wt.%) hybrid before immersion in 1.5 SBF

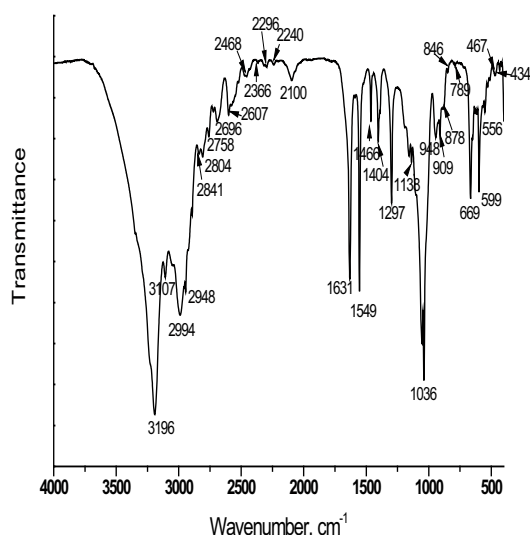


Figure 10. FTIR of the G/S 25:75 wt.% after immersion in SBF for 3 days

CO_3^{2-} modes) which can be assigned to -OH vibrational modes [24,61]. On the other hand, the stretching band at $\sim 3400\text{ cm}^{-1}$ due to the -OH was not observed after immersion for the hybrids in 1.5 SBF.

The information from FTIR spectra of the samples immersed in 1.5 SBF is summarized in Table 2.

3.5. SEM of the hybrids before and after immersion in 1.5 SBF for 3 days

SEM images obtained for G/S hybrids before immersion in 1.5 SBF are given in Figs. 11 and 12.

SEM morphology of the sample with high gelatine content (Fig. 11) shows relatively dense microstructure like that of the hydroxyapatite/gelatine nanocomposites prepared via co-precipitation method in the presence of different cross-linkers [18]. It is important to note that the silicocarnotite particles adhere in a non-homogeneous way on to the gelatine matrix, as presented in [67]. When the quantity of silicocarnotite in the hybrid increased to 75 wt.% (Fig. 12) we observe different silicocarnotite aggregates, which are composed of the glass-ceramic particles embedded in gelatine matrix [17]. As described in reference [12] SEM image also depicts the presence of hollow zones with various pore diameters (5 and 6.7 μm) and we also see that the silicocarnotite preserves its morphology in the conditions used. In accordance with our previous investigation [36], silicocarnotite thermally treated at $1200^\circ\text{C}/2\text{ h}$ could be ascribed as an non-densified sample. In agreement with other authors [68] we also observed that the densification of the silicocarnotites decreases with increasing silica content.

SEM images of G/S hybrids after immersion in 1.5 SBF are given in Figs. 13 and 14.

Fig. 13 shows SE-micrographs of the sample G/S (75:25 wt.%) after immersion in 1.5 SBF for 3 days. Consistent with the results reported by Durucan and Brown [69] the CO_3HA formed in flake-like morphology with smaller crystalline size. EDS of the sample gave Ca/P of 1.82. The observed Ca/P ratio (at.%) was

Table 2. IR vibration modes and their assignments observed for the G/S hybrids immersed in 1.5 SBF for 3 days

Vibration mode	IR for G/S (75:25 wt.%), cm^{-1}	IR for G/S (25:75 wt.%), cm^{-1}	Literature
$\nu_2 \text{PO}_4^{3-}$	479	467	[24, 62]
$\nu_3 \text{PO}_4^{3-}, \nu_{\text{as}} \text{O-Si-O}$	915	909, 948	[10, 17, 18, 55, 58]
$\nu_3 \text{PO}_4^{3-}$	1037	1036	[24, 58, 61]
$\nu_3 \text{PO}_4^{3-}$	1144	1138	[58]
$\nu_3 \text{PO}_4^{3-}$	1208	1201	[10, 17]
$\nu_3 \text{PO}_4^{3-}$	1296	1297	[64]
$\nu_4 \text{PO}_4^{3-}$	600	556, 599	[24, 58, 60, 62]
$\nu_2 \text{CO}_3^{2-}$	872	866, 878	[24, 58, 61, 62]
$\nu_3 \text{CO}_3^{2-}$	1404	1404	[53, 65]
$\nu_3 \text{CO}_3^{2-}$	1460	1466	[24, 62, 63]
$\nu_3 \text{CO}_3^{2-}$	1555	1549	[24, 61, 62]
$\nu_4 \text{CO}_3^{2-}, \text{OH}^-$	669	669	[24, 61]
$\nu_4 \text{CO}_3^{2-}$	692	692	[19, 24]
H_2O	1631	1631	[66]

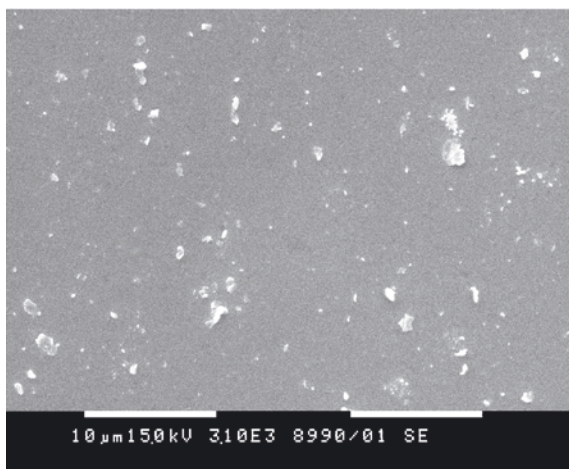


Figure 11. SEM of the G/S (75:25 wt.%) hybrid before immersion in 1.5 SBF

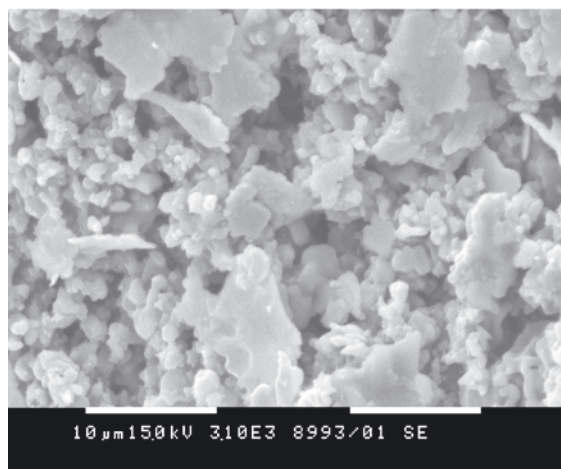


Figure 12. SEM of the G/S (25:75 wt.%) hybrid before immersion in 1.5 SBF

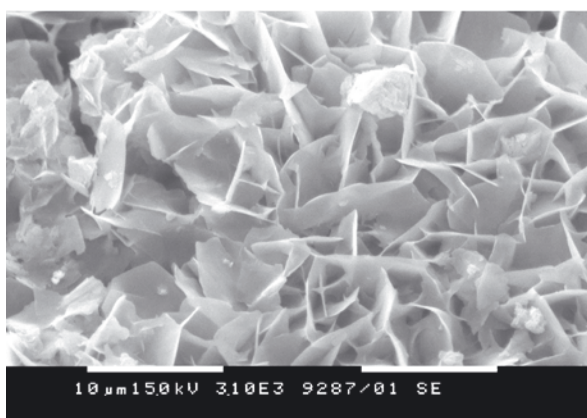


Figure 13. SEM of the G/S (75:25 wt.%) hybrid after immersion in 1.5 SBF

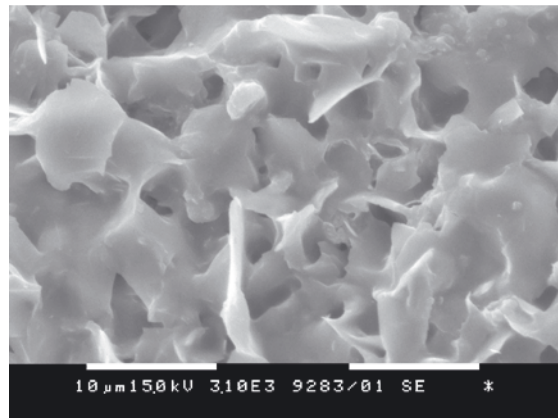


Figure 14. SEM of the G/S (25:75 wt.%) hybrid after immersion in 1.5 SBF

higher than the Ca/P ratio for the stoichiometric HA (C/P=1.67) and is due to the substitution of CO_3^{2-} for PO_4^{3-} [62]. For the G/S (25:75 wt.%) sample, SEM (Fig. 14) depicts that the surface of the sample is covered with calcium phosphate layer. EDS measurement showed a Ca/P=1.22. On the basis of this result we can assume that after immersion in 1.5 SBF amorphous calcium phosphate has been observed on the surface of the sample.

4. Conclusions

The aims of the present article were to prepare gelatin/silicocarnotite hybrid materials with different weight ratio of the components and to evaluate the *in vitro* bioactivity of the hybrids in 1.5 SBF. The silicocarnotite was prepared *via* polystep sol-gel method with Ca/P+Si (molar ratio) equal to 1.67. Water-soluble gelatin was mixed with silicocarnotite glass-ceramic powder in 25:75

and 75:25 wt.% without cross-linkage. The mixture obtained was readjusted to pH=8 with 25% NH_4OH . The hybrids so synthesized were dried at 37°C/12 h. The materials, before and after immersion in 1.5 SBF, were characterized by FTIR, XRD and SEM.

FTIR showed that the amide I peak, observed for pure gelatine centered at 1673 cm^{-1} shifted to 1669 cm^{-1} and to 1660 cm^{-1} for the hybrids. The “red shift” of amide I peak indicated that the C=O bonds in the peptide chain were weakened due to formation of new chelate bonds between Ca^{2+} and C=O bond. On the other hand, in the FTIR spectra before immersion in 1.5 SBF showed the presence of the bands centred at 1333 cm^{-1} and 1332 cm^{-1} . The presence of these bands could be ascribed to the formation of $\text{COO}^- \text{Ca}^{2+}$ bond in the hybrids prepared. The data presented were in a good agreement with X-ray diffraction analysis. After immersion of the hybrids in 1.5 SBF for 3 days, FTIR depicts the formation of, A- and B-type carbonate containing hydroxyapatite (A/B- CO_3HA) on the surface.

XRD shows the presence of hydroxyapatite with defined crystallinity. SEM/EDS showed calcium phosphates with different morphology on the samples immersed in 1.5 SBF for 3 days. XPS for the G/S hybrid with 25:75 wt.% after *in vitro* test for 3 days proved the presence of Ca-deficient hydroxyapatite.

References

- [1] M. Chang, R. DeLong, *Dental Materials* 25, 261 (2009)
- [2] L. Gineste *et al.*, *J. Biomed. Mater. Res.* 48, 224 (1999)
- [3] A. Clasen, I. Ruyter, *Adv. Dent. Res.* 11, 523 (1997)
- [4] Q. Liu, J. de Wijn, C.A. van Blitterswijk, *J. Biomed. Mater. Res.* 40, 257 (1998)
- [5] A. Wang *et al.*, *Appl. Surf. Sci.* 253, 3311 (2007)
- [6] W. Zhang, S. Liao, F. Cui, *Chem. Mater.* 8, 3221 (2003)
- [7] J. Song, V. Malathong, C. Bretozzi, *J. Am. Chem. Soc.* 127, 3366 (2005)
- [8] J. Song, E. Saiz, C. Bertozzi, *J. Am. Chem. Soc.* 125, 1236 (2003)
- [9] G. Wei, F. Ma, *Biomaterials* 25, 4749 (2004)
- [10] M. Chang, C. Ko, W. Douglas, *Biomaterials* 24, 2853 (2003)
- [11] K. Furucui, Y. Oaki, H. Imai, *Chem. Mater.* 18, 229 (2006)
- [12] S. Teng *et al.*, *Compos. Sci. Technol.* 66, 1532 (2006)
- [13] M. Chang, C. Ko, W. Douglas, *Biomaterials* 24, 3087 (2003)
- [14] M. Chen *et al.*, *Appl. Surf. Sci.* 254, 2730 (2008)
- [15] M. Chang, C. Ko, W. Douglas, *J. Mater. Sci.* 40, 2723 (2005)
- [16] W. Liu *et al.*, *J. Mater. Sci.* 41, 1851 (2006)
- [17] M. Chang, T. Ikoma, J. Tanaka, *J. Mater. Sci.* 39, 5547 (2004)
- [18] M. Chang, W. Douglas, *J. Mater. Sci.: Mater. Med.* 18, 2045 (2007)
- [19] J. Sundaram, T. Durance, R. Wang, *Acta Biomaterialia* 4, 932 (2008)
- [20] C. Shu *et al.*, *Ceramics International* 33, 193 (2007)
- [21] H-W. Kim, H-E. Kim, V. Salih, *Biomaterials* 26, 5221 (2005)
- [22] X. Liu *et al.*, *Biomaterials* 30, 2252 (2009)
- [23] M. Chang, *J. Mater. Sci.: Mater. Med.* 19, 2837 (2008)
- [24] E. Rosseeva *et al.*, *Chem. Mater.* 20, 6003 (2008)
- [25] A. Cios, B. Mycek, *Ceram. Int.* 27, 767 (2001)
- [26] M. Iio, M. Esaki, *J. Mater. Sci.: Mater. Med.* 10, 249 (1999)
- [27] T. Nordstrom *et al.*, *J. Biotechnol.* 69, 125 (1999)
- [28] S.-M. Lien, C.-H. Chien, T.-J. Huang, *Materials Science and Engineering C* 29, 315 (2008)
- [29] S. Panzavolta *et al.*, *Acta Biomaterialia* 5, 636 (2009)
- [30] K.-Y. Chen *et al.*, *Biomaterials* 30, 1682 (2009)
- [31] A. Ruys, *J. Aust. Ceram. Soc.* 29, 71 (1993)
- [32] Y.-J. Lee *et al.*, *J. Korean. Ceram. Soc.* 40, 1096 (2003)
- [33] S.-R. Kim *et al.*, *Key Eng. Mater.* 218-220, 85 (2002)
- [34] F. Balas, J. Perez-Pariente, M. Vallet-Regi, *J. Biomed. Mater. Res.* 66A, 364 (2003)
- [35] J. Reid *et al.*, *Biomaterials* 26, 2005 (2005)
- [36] L. Radev *et al.*, *Cent. Eur. J. Chem.* 7, 317 (2009)
- [37] L. Radev *et al.*, *Cent. Eur. J. Chem.* 7, 322 (2009)
- [38] V. Hristov *et al.*, *Cent. Eur. J. Chem.* (in press)
- [39] L. Radev *et al.*, *Cent. Eur. J. Chem.* (in press)
- [40] R. Reis *et al.*, *J. Mater. Sci.: Mater. Med.* 8, 897 (1997)
- [41] M. Ferraz *et al.*, *J. Mater. Sci.: Mater. Med.* 12, 629 (2001)
- [42] B. Samuneva *et al.*, *J. Sol-Gel Sci. Technol.* 26, 273 (2003)
- [43] Y. Ivanova *et al.*, *Cent. Eur. J. Chem.* 7, 42 (2009)
- [44] Y. Ivanova *et al.*, *Thin Solid Films* 515, 271 (2006)
- [45] B. Samuneva *et al.*, *J. Non-Cryst. Solids* 354, 733 (2008)
- [46] G. Falini, M. Gazzano, A. Ripamonti, *J. Mater. Chem.* 10, 535 (2000)
- [47] W. Zhang *et al.*, *J. Am. Ceram. Soc.* 86[6], 1052 (2003)
- [48] K. Pal, A. Banthia, D. Majumdar, *AAPS Pharm. Sci. Tech.* 8[1], E1 (2007)
- [49] M. Santos, L. Hemeine, H. Mansur, *Mater. Sci. Eng. C* 28, 563 (2008)
- [50] K. Payne, A. Vies, *Biopolymers* 27, 1749 (1988)
- [51] S. Krimm, J. Bandekar, *Adv. Protein Chem.* 38, 181 (1986)
- [52] J. Vandiver *et al.*, *J. Biomed. Mater. Res.* 78A, 352 (2006)
- [53] I. Rehman, W. Bonfield, *J. Mater. Sci.: Mater. Med.* 8, 1 (1997)
- [54] A. Martines, I. Izquierdo-Barba, M. Vallet-Regi, *Chem. Mater.* 12, 3080 (2000)

Acknowledgements

The financial support of the Bulgarian NSF under contract № VU-TN-102/2005 is gratefully acknowledged.

- [55] I. Gibson, S. Best, W. Bonfield, J. Biomed. Mater. Res. 44, 422 (1998)
- [56] J. Roman, S. Padila, M. Vallet-Regi, Chem. Mater. 15, 798 (2003)
- [57] X. Yang et al., Mater. Sci. Eng. C 29, (2009)
- [58] B. Gaihre et al., Mater. Sci. Eng. C 28, 1297 (2008)
- [59] Z. Yang et al., J. Mater. Chem. 15, 1807 (2005)
- [60] K. Mohamed, A. Mostafa, Mater. Sci. Eng. C 28, 1087 (2008)
- [61] M. Chang, W. Douglas, J. Tanaka, J. Mater. Sci.: Mater. Med. 17, 387 (2006)
- [62] Y. Yusufogly, M. Akinc, J. Am. Ceram. Soc. 91[10], 3147 (2008)
- [63] Y. Suetsugu, I. Shimoya, J. Tanaka, J. Am. Ceram. Soc. 81[3], 746 (1998)
- [64] G.A. Stanciu et al., J. Biomed. Pharm. Eng. 1[1], 34 (2007)
- [65] N. Higon et al., Chem. Mater. 1451 (2004)
- [66] I. de Lima, A.M. Costa, I.N. Bastos, Mater. Res. 9, 1 (2006)
- [67] F. Boccafoschi et al., Biomaterials 26, 7410 (2005)
- [68] M. Vallet-Regi, D. Arcos, J. Mater. Chem. 15, 1509 (2005)
- [69] C. Durucan, P. Brown, J. Mater. Sci.: Mater. Med. 11, 365 (2000)